Slepton production from gauge boson fusion

Debajyoti Choudhury,[1] Anindya Datta,[2] Katri Huitu,[2] Partha Konar,[1] Stefano Moretti,[3] and Biswarup Mukhopadhyaya[1]
[1]*Harish-Chandra Research Institute, Chhatnag Road, Jhusi, Allahabad 211 019, India*
[2]*Helsinki Institute of Physics, and Division of High Energy Physics, Department of Physical Sciences, P.O. Box 64, 00014 University of Helsinki, Finland*
[3]*Department of Physics & Astronomy, University of Southampton, Highfield, Southampton SO17 1BJ, United Kingdom*
(Received 25 April 2003; published 24 October 2003)

We emphasize that charged slepton pairs produced via vector-boson fusion along with two high-mass, high-p_T forward and backward jets (in two opposite hemispheres) can have a higher production cross section for heavy slepton masses than that from conventional Drell-Yan production at a hadronic collider such as the CERN LHC. We analyze the signal and leading backgrounds in detail in the minimal supersymmetric standard model with conserved baryon and lepton numbers. Our investigation reveals that the mass reach of the vector-boson fusion channel is certainly an improvement over the scope of the Drell-Yan mode.

DOI: 10.1103/PhysRevD.68.075007 PACS number(s): 12.60.Jv, 13.85.Rm

I. INTRODUCTION

Vector-boson fusion (VBF) at hadronic machines such as the Large Hadron Collider (LHC) at CERN has been suggested as a useful channel for studying Higgs boson signals. The characteristic features of this mechanism are two highly energetic quark jets, produced in the forward and backward directions in opposite hemispheres of the detector and carrying a large invariant mass. The absence of color exchange between these two jets ensures a suppression of hadronic activity in the central region [1], contrary to the case of typical QCD backgrounds. Though it was originally proposed as a signal for a heavy Higgs boson [2,3], the usefulness of the VBF channel in detecting an intermediate mass Higgs boson has also been subsequently demonstrated [4].

Some recent works [5] have further pointed out the effectiveness of this channel in the context of new physics searches, particularly for new particles that do not interact strongly. Perhaps the best example is afforded by supersymmetric theories, wherein conventional search strategies for neutralinos and charginos may run into difficulties, at least for a significant part of the parameter space. Encouraged by the success of the VBF channel in exploring such cases, we investigate here its efficacy in the search for the supersymmetric partners of the leptons, namely, the sleptons ($\tilde{\ell}$). This is of particular interest as the conventional search strategies for such particles at the LHC are not very promising, especially for slepton masses above 300 GeV or so. In fact, direct pair production of sleptons via the Drell-Yan (DY)process has been investigated extensively in the literature [6,7]. At the Fermilab Tevatron and the LHC, the corresponding next-to-leading order (NLO) production cross sections fall below 1 fb for slepton masses above 200 and 500 GeV, respectively [7]. Within, e.g., the minimal supergravity (MSUGRA) scenario, such sleptons would decay mainly into a charged lepton (ℓ) and the lightest neutralino ($\tilde{\chi}_1^0$), thus resulting in an opposite-sign dilepton pair with missing energy.[1] As can be expected, the upper limit of the corresponding mass reach is quite low ($\sim$250 GeV at the LHC) [6].

In the present work, we want to investigate whether the above mass limit can be improved at the LHC when we use the VBF channel for slepton production. Slepton pair production via *WW* fusion has been discussed earlier in Ref. [9], and more recently, in the special context of anomaly mediated SUSY breaking, in [10]. It is needless to mention that the VBF channel is suppressed by four powers of $g_{\rm EW}$, the electroweak (EW) coupling, with respect to the DY mode. However, for the latter, the cross section falls rather fast with the slepton mass, whereas one should expect a milder dependence on $m_{\tilde{\ell}}$ in VBF. We will only consider pair production of charged sleptons ($\tilde{\ell}_L$, $\tilde{\ell}_R$) along with two forward and backward jets. In most of the following analysis, we will assume the general minimal supersymmetric standard model (MSSM) with parameters defined at the EW scale, as we will not adhere to any particular SUSY-breaking scenario and make no assumption related to any high mass scale physics other than adopting gauge coupling unification. This implies that whereas the slepton masses are free parameters in our analysis, the neutralino masses and couplings are completely specified by the $SU(2)$ gaugino mass M_2, the Higgs(ino) mass parameter μ and $\tan\beta$, the ratio of the two Higgs vacuum expectation values arising in the MSSM. The only constraints on this set of parameters are the experimental ones, most notably those imposed by the LEP analyses. At the very end, we will try to correlate our results to the MSUGRA parameter space.

The plan of the article is as follows. In Sec. II, we will discuss in detail the nature of the proposed signal and its various features. Section III will be devoted to a discussion

[1]Slepton pair production has also been investigated in the case of gauge mediated supersymmetry (SUSY) breaking [8] where the third generation of sleptons has a very distinct decay signature.

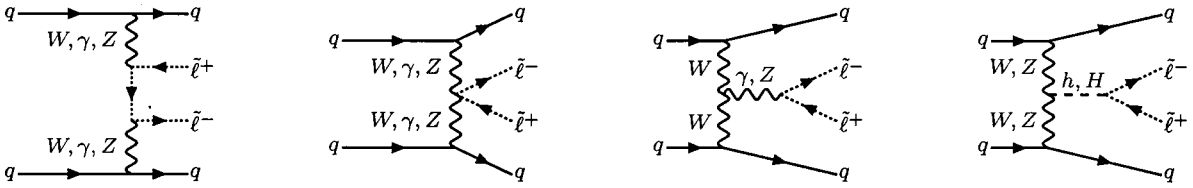

FIG. 1. Generic parton level diagrams leading to slepton pair production through electroweak VBF at hadronic colliders.

of the event selection criteria adopted here, while the end results, embodied in a set of discovery contours, are reported in Sec. IV. We summarize and conclude in Sec. V.

II. THE SIGNAL

A. Slepton pair production

We begin by considering slepton pair production through VBF. The generic (lowest-order) diagrams contributing to this process are depicted in Fig. 1, where each of the q's represents either a quark or an antiquark. Clearly, such diagrams do not exhaust the entire set of contributions to the process $q_1 q_2 \to q_3 q_4 \tilde{\ell}\tilde{\ell}^*$. In fact, apart from a host of other EW diagrams, one also has to include those involving a gluon exchange. In addition, although they do not interfere with the signal, one also has to consider graphs with gluons in either of the initial and final state. Although we shall impose kinematic constraints to ensure that diagrams such as those in Fig. 1 dominate overwhelmingly, in the actual computation, one still needs to include the full set of diagrams that lead to a slepton-pair accompanied by two jets. In doing so, we limit ourselves to a tree-level calculation and use the HELAS subroutines [11] to numerically evaluate the ensuing helicity amplitudes. For our parton-level Monte Carlo analysis, we use the CTEQ4L parton distributions [12] with the scale set at the slepton mass ($m_{\tilde{\ell}}$).

The very structure of the VBF diagrams immediately suggests that such contributions would be largely concentrated in kinematic regions where the vector bosons are nearly on mass shell. This translates into two rather forward and backward jets, one in each hemisphere. Since no colored particle is exchanged, the rapidity gap between these forward and backward jets would be essentially free of hadronic activity. Thus we start by characterizing the signal in terms of the following basic criteria:

(a) The sleptons (and their decay products) are entirely contained in the rapidity regime in between the two forward and backward jets, labeled as j_i $(i=1,2)$, satisfying the following requirements:

$$2 \leqslant |\eta(j_i)| \leqslant 5, \quad \eta(j_1)\,\eta(j_2) < 0. \tag{1a}$$

(b) Both jets should have sufficient transverse momentum to be detected, namely,

$$p_T(j_i) \geqslant 15 \ \text{GeV}. \tag{1b}$$

(c) The invariant mass of the pair of forward jets should be sufficiently large,

$$M_{j_1 j_2} > 650 \ \text{GeV}. \tag{1c}$$

(d) There should be no hadronic activity in the rapidity interval between these two jets.

We have explicitly checked that, on imposition of the above criteria, the resulting cross section is overwhelmingly dominated by the VBF diagrams. It should further be remembered that these are only our ''basic cuts,'' and serve the purpose of establishing the characteristics of a VBF event. However, as we shall see shortly, additional cuts are required to enhance the visibility of the signal against backgrounds. While, in our analysis, these criteria have been imposed at the parton level, they are expected to mimic actual detector events even after hadronization is incorporated. Experimentally, criterion (d) is implemented by applying a central jet veto. The above cuts select signal events whose survival probability against such a veto turns out to be between 80 to 90 percent [13]. For *real emission correction to DY-type processes* (which involve color exchange between the jets), in contrast, the corresponding survival probability is below 30 percent [14]. In the remainder of our analysis, we will include the full set of contributions, weighed appropriately by the respective survival probabilities.

Let us now examine the total production cross section and the possible parameter dependences of the signal process. Since we shall concentrate only on the sleptons of the first two generations ($\tilde{e}_{L,R}$ and $\tilde{\mu}_{L,R}$), the Higgs mediated diagrams in Fig. 1 are not important. This also implies that the production cross section is not sensitive to either μ, $\tan\beta$ or the slepton mixing.[2] Thus the production cross section is essentially model-independent and is determined solely by the slepton mass $m_{\tilde{\ell}}$. In Fig. 2, we display this functional dependence. The lowest order DY cross section (without any cuts) is also shown for an approximate comparison of the relative magnitude. A few points are immediately obvious.

Formally, our cross section is suppressed by two powers of $\alpha_{\rm em}(\alpha_{\rm weak})$ when compared to the DY one. This is reflected in the dominance of the DY rates for small slepton masses.

The cross-section falloff with mass is much slower for the VBF process, as compared to the DY mode, as intimated. This can be understood by recognizing that the DY cross section suffers from the presence of an s-channel propagator. In contrast, the VBF process could be viewed in terms of an effective $\gamma/Z/W$ approximation, wherein the large logarithms associated with the emission of a ''nearly massless'' gauge boson compensate for the extra factors of $\alpha_{\rm em}(\alpha_{\rm weak})$. Notice however that such logarithmic enhancements are fi-

[2]However, as we shall see later, μ plays a significant role in slepton decays and affects then the signal as a whole.

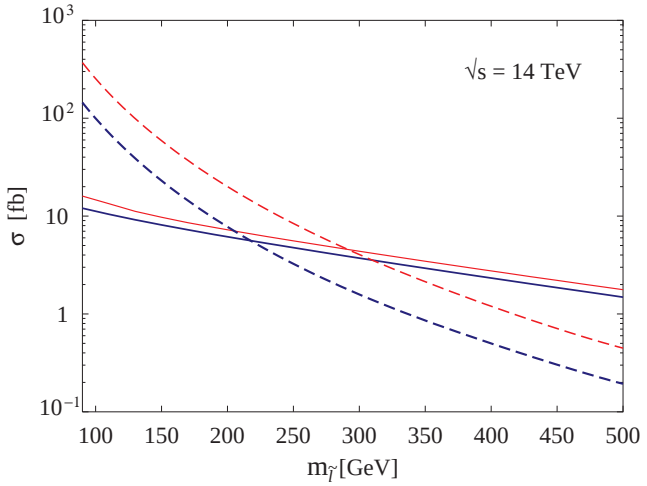

FIG. 2. The total cross section (solid lines) for slepton pair production at the LHC in association with two forward jets. The cuts of Eqs. (1a)–(1c) have been imposed on the VBF rates. The CTEQ4L parton distributions have been used with the factorization scale set at $m_{\tilde{\ell}}$. The dashed curves represent the corresponding DY cross sections. In each case, the upper and lower curves correspond to $\tilde{\ell}_L$ and $\tilde{\ell}_R$ (one flavor) respectively.

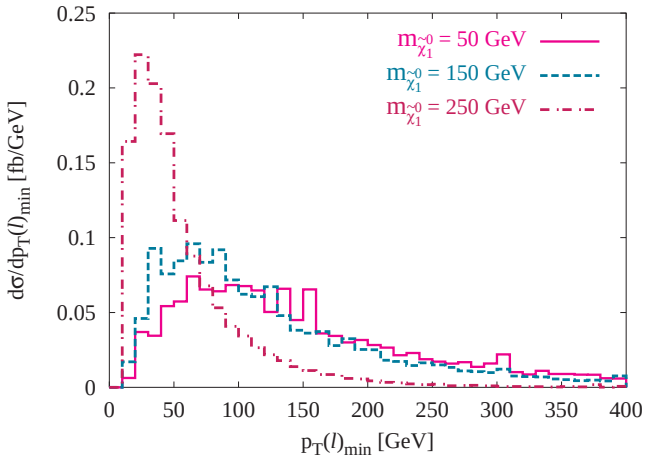

FIG. 3. The distribution of the softer of the two lepton p_T's for three different values of the LSP mass and a fixed slepton mass of 300 GeV.

nite and well under control (that is, they do not need a higher order treatment) since the requirements of forward and backward jet tagging that we will put in place (a minimum p_T together with a maximal rapidity) act as effective regulators, on the same footing as in Refs. [2–4].

The VBF process is dominated by the photon diagrams. This is to be expected in view of the previous remark and is reflected by the relatively small ($\leqslant 10\%$) fractional difference in the cross sections for $\tilde{\ell}_L$ and $\tilde{\ell}_R$ production.

As Fig. 2 also shows, the VBF cross section is significantly larger than the DY one for large values of $m_{\tilde{\ell}}$. Since this is precisely the region of the parameter space where the DY production mode is of little use, it behooves us to investigate the VBF channel further. In addition, the two forward and backward jets are peculiar to this channel and could serve to eliminate backgrounds.

B. Slepton decay modes and kinematics

Once produced, the sleptons will decay into either a chargino-neutrino pair or into a neutralino-lepton pair. The partial decay widths are governed by both the mass and composition of the charginos (neutralinos) as well as the handedness of the slepton (L or R). As is well known, as long as R-parity is conserved, the lightest supersymmetric particle (LSP) is stable. Since consistency with observations demands that the lightest neutralino be the LSP, the latter is invisible and all other supersymmetric particles decay into it. Thus the slepton decay must result in *same-flavor opposite-sign dilepton pairs associated with missing transverse momentum*. Cascade decays through the heavier neutralinos or charginos would produce a similar signature (with still more particle tracks in the detector), so that they may be deemed as part of the signal. However, for reasons explained later, we will primarily be concentrating on the direct decay of the slepton into the lepton-LSP pair. As we have mentioned in Sec. II A, we would be requiring the *lepton pair to lie within the rapidity interval between the jets*. In other words ($i=1,2$),

$$|\eta(\ell_i)| \leqslant 2. \tag{2a}$$

Of course, the two leptons must have enough transverse momenta to be detectable:

$$p_T(\ell_i) \geqslant 15 \ \text{GeV}. \tag{2b}$$

Before we decide on further selection criteria, it is useful to examine the signal profile resulting from the production of a slepton pair of a given mass and decaying into a particular neutralino, again of a given mass. A variable of interest here is the smaller of the two lepton transverse momenta, namely, $\min[p_T(\ell_1), p_T(\ell_2)]$. In Fig. 3, we display the distribution in this observable for a given slepton mass and three representative values of the LSP mass. Note that a smaller value of $m_{\tilde{\ell}} - m_{\tilde{\chi}_1^0}$ softens this distribution. This is to be expected. Since the sleptons prefer to be produced with little transverse momenta, a high p_T for the decay products would only be possible if the mass difference were large. A similar pattern would appear in the case of the missing transverse momentum.

This also explains partly our "neglect" of cascade decays through the heavier neutralinos and charginos. The final states resulting from such decay channels typically contain additional leptons or jets. To avoid QCD backgrounds, we would need to concentrate on the multilepton modes. Such decay patterns, however, occur less frequently than those involving quarks (and hence additional jets). Moreover, with a smaller mass difference between the slepton and a heavier neutralino or chargino, the primary lepton would tend to be softer and hence often evade the selection process. Explicit computation shows that the inclusion of the cascade decays

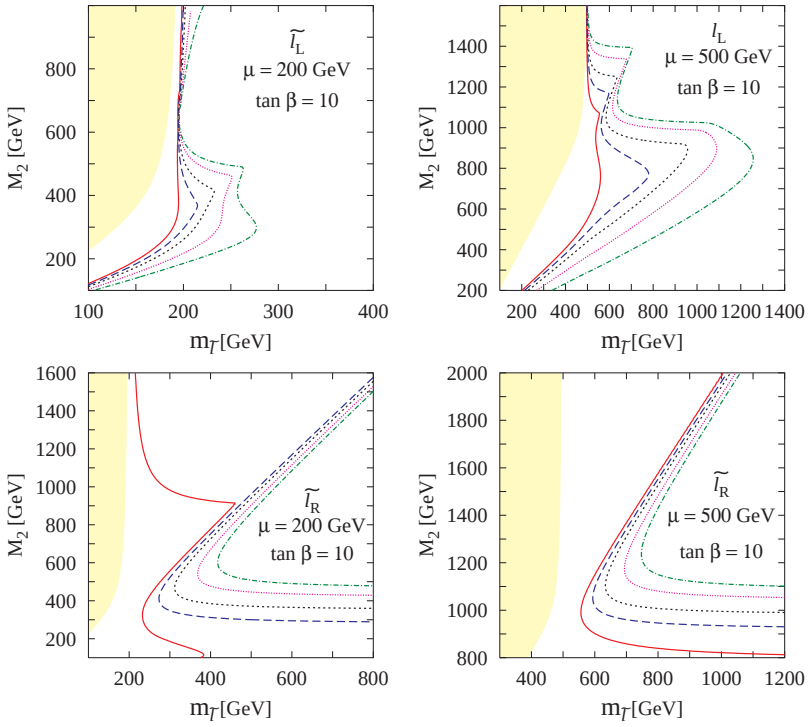

FIG. 4. Contours for constant $BR(\tilde{\ell} \to \tilde{\chi}_1^0 + \ell)$ for both $\tilde{\ell}_L$ (upper panels) and $\tilde{\ell}_R$ (lower panels) in the $m_{\tilde{\ell}}$-M_2 plane. In each case, the left and right panels correspond to $\mu = 200$ GeV and 500 GeV, respectively. The shaded area corresponds to the part of the parameter space that leads to the slepton being the LSP. The contours, from left to right, are for $BR(\tilde{\ell} \to \tilde{\chi}_1^0 + \ell) = 0.9$, 0.7, 0.5, 0.3 and 0.2, respectively.

can result in only a marginal improvement of our results and we shall ignore their effects henceforth.

C. Slepton branching fractions

We now turn to the issue of the slepton branching ratio (BR) into the lightest neutralino. This depends on quite a few parameters: $m_{\tilde{\ell}}$, μ, $\tan\beta$ and the gaugino mass parameters M_1 and M_2. Of these, the dependence on $\tan\beta$ is the least pronounced and therefore we shall henceforth use only one value of it, namely, 10. Furthermore, to reduce the number of parameters, we shall assume the unification relation between M_1 and M_2. Thus, only three parameters remain, namely $m_{\tilde{\ell}}$, μ and M_1. For a given slepton mass, the relevant branching fraction is then governed by essentially two factors: (i) the composition of the LSP and (ii) whether decays into the heavier neutralinos or charginos are allowed. The resulting dependence is still quite intricate as can be gauged from Fig. 4, where we present iso-branching fraction contours in the $m_{\tilde{\ell}}$-M_2 plane for two positive values of μ. A set of conclusions follow immediately.

For a given mass, the $\tilde{\ell}_R$ has a larger probability for decaying directly into the LSP as compared to the $\tilde{\ell}_L$. This effect is even more pronounced for larger μ and can be understood from the fact that whereas the $\tilde{\ell}_R$ has no coupling to the $\tilde{W}^{\pm,0}$ eigenstates, it is precisely these states that the $\tilde{\ell}_L$ preferentially decays into.

For $\mu < M_2$, the two lightest neutralinos and the lighter chargino are often Higgsino-dominated. Selectrons and smuons then tend to cascade through the heavier neutralinos (heavier chargino). However, this possibility is curtailed when M_2 is large so that kinematic accessibility of these states is denied.

When μ and M_2 are comparable, the relative weight of the *B*-ino and Higgsino states in the LSP controls the BR of sleptons decaying into it.

As we have already seen (Fig. 2), the production cross sections for $\tilde{\ell}_L$ and $\tilde{\ell}_R$ are very similar, with the former being slightly larger. However, with the $\tilde{\ell}_R$ decaying into the LSP much often, it is expected that, for identical masses, it is this $(\tilde{\ell}_R \tilde{\ell}_R^*)$ production channel that will finally dominate the signal.

D. Signal profile and parameter dependence

Before we end this section, we would like to discuss the interplay of the kinematic effects between the slepton-LSP mass difference (as exemplified by Fig. 3) and the branching fractions. In doing this we shall assume that the two sleptons $\tilde{\ell}_{L,R}$ are degenerate, a very good approximation in SUGRA-inspired scenarios. In Fig. 5, we demonstrate the dependence of the cross section on the slepton mass for three representative values of M_2. For $m_{\tilde{\ell}} \gg M_2$, the $\tilde{\ell}_R$ decays predominantly into the LSP while the $\tilde{\ell}_L$ is allowed more channels. The important point, however, is that, in this limit, the branching fraction into the LSP is essentially independent of M_2. Moreover, with a large separation between $m_{\tilde{\ell}}$ and $m_{\tilde{\chi}_1^0}$, the leptons acquire transverse momenta sufficiently large (Fig. 3) to satisfy the selection criteria. Thus, in this regime, the cross section is practically independent of M_2 and is determined solely by $m_{\tilde{\ell}}$. For very low values of $m_{\tilde{\ell}}$, on the other hand, the aforementioned kinematic dependence on the mass difference becomes very important: the larger M_2 is, the smaller is the average value of $p_T(\ell)$, resulting in the suppression of the signal (Fig. 5). And finally, the very sharp

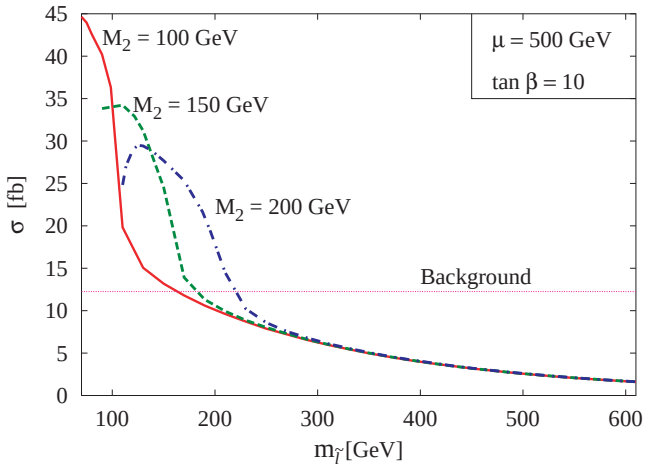

FIG. 5. Variation of the signal cross section with the slepton mass for some representative values of M_2 and given μ and $\tan\beta$. The corresponding LSP masses are $m_{\tilde{\chi}_1^0}=48.8$, 73.6, 98.4 GeV respectively. Only the basic cuts of Eqs. (1a)–(1c), (2a), (2b) have been imposed. Also shown is the corresponding background cross section.

decrease in the signal strength for $m_{\tilde{\ell}} \gtrsim M_2$ can be traced to the rapid change of the branching fraction into the LSP on account of new channels opening up.

III. BACKGROUNDS AND THEIR ELIMINATION

Same-flavor, opposite-sign dilepton and missing energy signals at the LHC can be faked by standard model (SM) processes where two opposite-sign W's or τ's are produced with two forward and backward jets, with the W's or τ's decaying leptonically. There is also a source of reducible background from ZZ production in the presence of initial state radiation. Here, however, an invariant mass cut on the lepton pair can remove the latter background almost completely. The continuum production due to an off-shell Z going to leptons is too small to be of any consequence. Production of $t\bar{t}$ pairs with subsequent semileptonic decays of top quarks can also produce the dilepton + jets + missing transverse energy final state. We can easily get rid of this background though, by remembering that the jet associated with top decay is always a b-jet. Such backgrounds are appreciable only for $|\eta_j| \leqslant 3$. Thus they can be eliminated with a b-veto if the b-trigger works up to such a rapidity. The pair production of charged Higgs bosons in VBF [16] can also yield opposite-sign dileptons with missing transverse momentum and forward and backward jet activity. This noise may be particularly dangerous, as it has the same topology of the signal, including the reduced hadronic activity in the central region. However, electrons and muons can emerge from charged Higgs boson decays only indirectly via τ's, and hence with a leptonic BR suppression and in flavor combinations of equal probability. In the end, we have explicitly checked, by varying the Higgs boson mass and the other relevant supersymmetric parameters consistently with the signal, that this background is not very large in general, so that we need not consider it any further. In summary, the

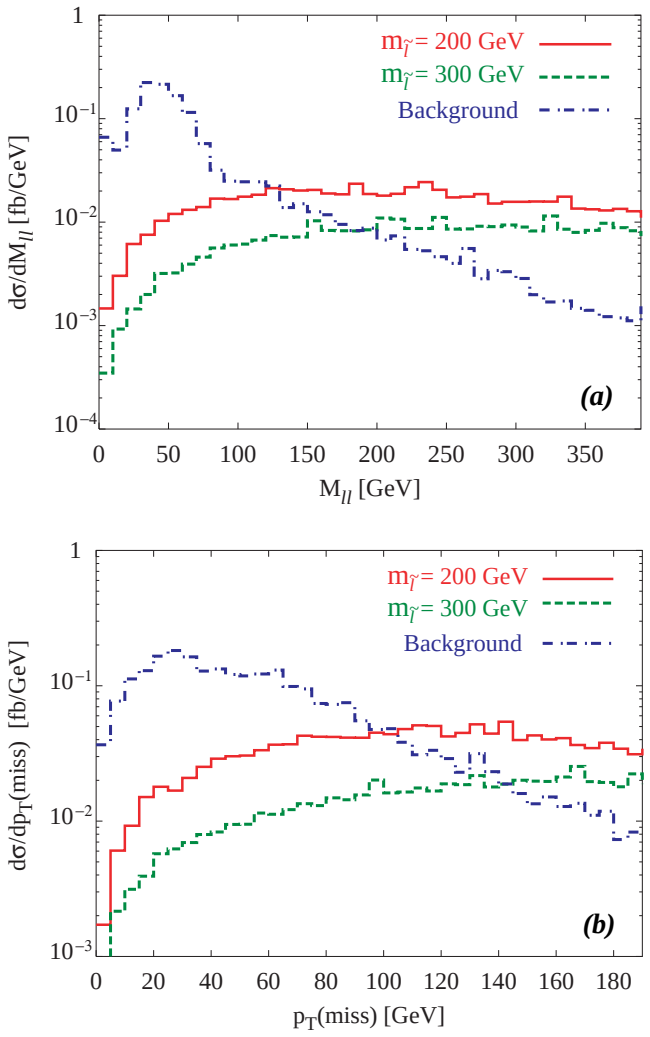

FIG. 6. (a) Invariant mass $M_{\ell\ell}$ and (b) missing transverse momentum p_T(miss) distributions for the signal for $M_2=150$ GeV, $\mu=500$ GeV, $\tan\beta=10$, $m_{\tilde{\ell}}=200,300$ GeV. Also shown are the corresponding background distributions.

dominant contributions to the background come from W's and (direct) τ's in almost equal strength, although some sizable effect is unavoidable from real emission corrections to the DY process, despite its moderate central jet veto survival probability. We have estimated all these backgrounds using the package MADGRAPH [17]. With the cuts described above, the missing transverse momentum and opposite sign dielectron and dimuon total background comes out to be about 13 fb (choosing the factorisation scale at $2M_W$), which we represent by the horizontal line in Fig. 5. Assuming that the b-veto will work up to $\eta=3$, the background gets contributions on the order of 8.5 fb and 4.5 fb from $\tau\tau$ and WW, respectively. In the following we will see that the background level can be reduced significantly with a minimal sacrifice of the signal by exploiting suitable kinematic distributions.

We examine the spectra in invariant mass [Fig. 6(a)] of the dilepton pair as well as in missing transverse energy [Fig. 6(b)] for both the signal (for some illustrative values of $m_{\tilde{\ell}}$ and $M_{\rm LSP}$) and the combined backgrounds after the previously mentioned cuts, and observe that:

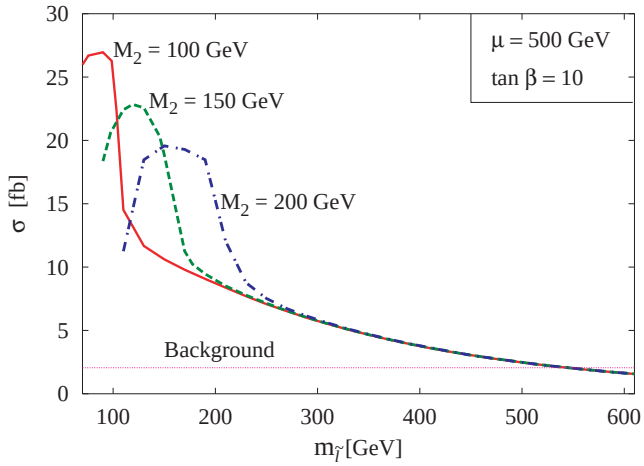

FIG. 7. As in Fig. 5, but now the cuts of Eqs. (3a)–(3c) have been imposed as well.

The invariant mass of the dilepton pair has a much harder spectrum for the signal as compared to the total background.

The missing transverse momentum distribution is harder for the signal, with the peaks shifting to higher values for lower masses of the LSP, once the slepton mass is fixed.

Keeping all this in mind, we impose a few additional selection criteria. For one, an event must be accompanied by a substantial missing transverse momentum:

$$p_T(\text{miss}) \geqslant 50 \ \text{GeV}. \tag{3a}$$

Furthermore, while the invariant mass for the dilepton pair should be sufficiently large to remove most of the background, i.e.

$$M_{\ell\ell} \geqslant 60 \ \text{GeV}, \tag{3b}$$

it should nevertheless be well away from the Z mass (in order to eliminate backgrounds accruing from $pp \to jjZ\nu_i\overline{\nu_i}$):

$$|M_{\ell\ell} - M_Z| > 5\Gamma_Z. \tag{3c}$$

These extra cuts have only a moderate effect on the signal while reducing the background down to only ~ 2 fb, as is evident from Fig. 7. As for the signal, the effects of the new kinematic cuts are more pronounced for low mass sleptons. If we increase the neutralino mass, the missing energy spectrum becomes harder while the dilepton mass distribution becomes softer. One can see by comparing Figs. 5 and 7 that, for $m_{\tilde{\ell}} \sim 100$–$200$ GeV, such a tradeoff has affected the $M_2 = 100$ GeV case most severely.

It should also be mentioned here that the characteristic signals of sleptons studied by us are subject to vitiation by other SUSY processes, such as cascades from squarks, gluinos and electroweak gauginos, leading to a potential ''residual SUSY background.'' As has already been noted in the first reference of [5], the squark or gluino background can be suppressed by the invariant mass cut on the forward jet pair. Furthermore, a veto against central hadronic activities is also helpful in eventually suppressing fake signals from squarks and gluinos. As for electroweak gauginos, in general their contributions to the signals under scrutiny have been found to be smaller [5], mostly due to suppression by the leptonic branching ratios of gauginos,[3] and the requirement that both leptons in the final state be of the same flavor. One situation where gauginos can intervene is when they can decay into *real sleptons*. Such a case, however, again leads to characteristic signals of the sleptons themselves, and therefore our estimate, if anything, is of a conservative nature.

As has already been mentioned, one has to multiply the signal rates with the central jet veto survival probability. This is a source of theoretical uncertainty in the predictions; we have used as our guidelines the results given in Ref. [14] for the survival probabilities for electroweak and QCD processes, already noted in Sec. II A. These probabilities pertain to a central jet with a minimum p_T of 20 GeV, which therefore translates into a definition of hadronic activities in the central region. For further discussion on the subject, the reader is directed to Ref. [15].

IV. DISCOVERY CONTOURS

We are now in a position to predict the potential of our channel to explore or exclude the supersymmetric parameters involved in this analysis. In Fig. 8, we present some significance contours of the predicted signals in the $M_2 - m_{\tilde{\ell}}$ plane for two values of μ. The shaded regions in the contour plots are either disallowed by the LEP data or inconsistent with the hypothesis that the lightest neutralino is the LSP. To calculate the significance ($\equiv S/\sqrt{B}$) we have assumed an integrated luminosity of 30 fb^{-1}. With 2.05 fb of total background cross section, this implies 40 signal events for 5σ discovery.

Evidently, the contours reflect rather promising statistics over a large region of the parameter space. The detailed nature of the contours are mostly governed by features related to slepton production and decay, which have been discussed in the previous sections. While there is a complex interplay of different factors, we would like to recall at this stage a few salient points which have roles to play in the predictions:

The slepton production rates decrease with increasing slepton mass.

The composition of the LSP as well as the other neutralinos and charginos is a deciding factor.

The mass difference between the slepton and the LSP determines the hardness of the resulting leptons and therefore the survival probability of the events against cuts.

As has been discussed earlier, while the right sleptons decay overwhelmingly into a B-ino-dominated LSP, the left ones often tend to cascade through the $SU(2)$ coupling.

The characteristic turning around of the curves for $\mu = 200$ GeV can also be seen for $\mu = 500$ GeV for higher values of M_2 and $m_{\tilde{\ell}}$.

The study of this signal also allows one to draw significance contours in the parameter space of an MSUGRA theory. For the purpose of illustration we have chosen μ

[3]A probable caveat is offered by a spectrum wherein the squarks are very heavy, while sleptons are only somewhat heavier than gauginos (with μ being relatively large).

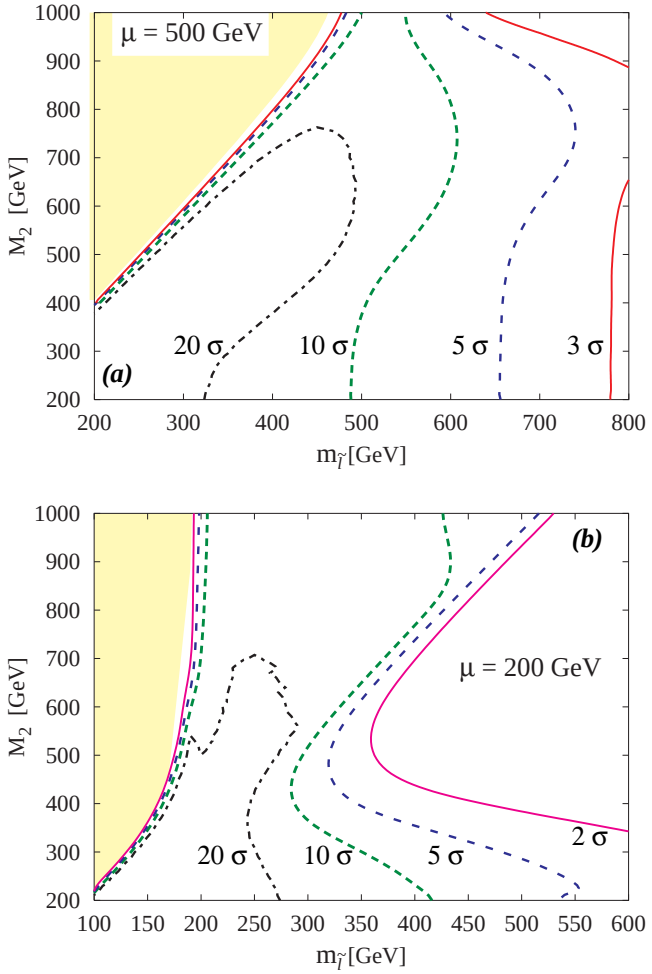

FIG. 8. Contours of constant significance in the $M_2-m_{\tilde{\ell}}$ plane for (a) $\mu=500$ GeV and (b) $\mu=200$ GeV, with $\tan\beta=10$.

>0, $A_0=0$ (always with $\tan\beta=10$), where A_0 is the trilinear SUSY-breaking parameter at the unification scale. In Fig. 9, the significance contours are presented for three values of $S/\sqrt{B}$. We do not present the results for $\mu<0$; it has already been stressed that the sign of μ has very little effect on either the slepton pair-production cross section or the slepton decay BR to the LSP. The effects of slepton mixing or $\tan\beta$ are also negligible, since we are considering sleptons of the first two generations. We also assume radiative EW symmetry breaking.

The dissimilarity between the contours of Fig. 9 and Figs. 8 might seem puzzling at first. However, an analytical study of the parameter space dependence immediately reveals the cause. Increasing m_0 (common scalar mass at the unification scale), results in an increase in the values of $m_{\tilde{\ell}}$ and μ. The consequent (modest) enhancement of the branching ratio into the LSP is, however, more than offset by the decrease in the production cross section due to higher slepton mass, and by the opening of additional decay channels into higher neutralinos or charginos, so long as $m_{1/2}$ is on the lower side. It should be noted that such channels (such as those into the second lightest neutralino and the lighter chargino) affect the left sleptons more in the form of reduced signal rates. In-

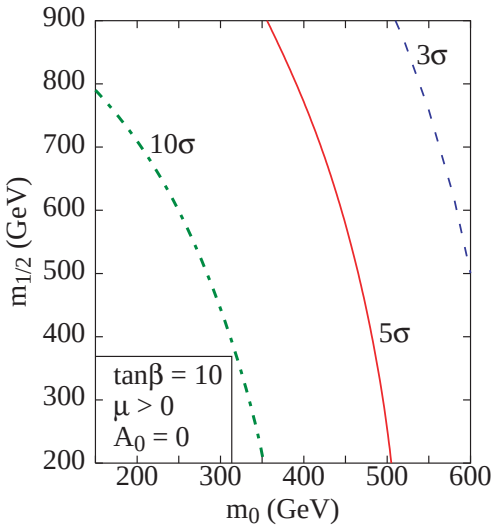

FIG. 9. Contours of constant significance in the $M_{1/2}-m_0$ plane for $\mu>0$, $A_0=0$ and $\tan\beta=10$. An integrated luminosity of 30 fb^{-1} has been assumed.

creasing $m_{1/2}$ (the common gaugino mass at the unification scale), on the other hand, has a twofold effect. First, it increases the LSP mass thus affecting the decay kinematics. More importantly, it also increases the slepton masses, preferentially that of the left sleptons. Since the latter suffer $SU(2)$ interactions (unlike their right-handed counterparts), their mass increases with $m_{1/2}$ at a faster rate. As a consequence, within this framework, the production rate for the left sleptons falls faster with an increasing $m_{1/2}$ than is the case for the right sleptons [18]. Finally, for most of the parameter space depicted in Fig. 9, the branching ratio for the right sleptons into the LSP is nearly unity, whereas the corresponding one for the left sleptons is a rather sensitive function of $(m_0-m_{1/2})$. Together, these two factors result in the signal strength being dominated by the contribution from the right sleptons. Moreover, with the decay kinematics playing a relatively subservient role, the signal is determined largely by the mass of the right-handed slepton alone. Thus the contours in Fig. 9 largely reflect the behavior of right sleptons, particularly when m_0 and $m_{1/2}$ are on the higher side.

For the kind of signal we are proposing, it is very crucial to know the background normalization very accurately, as one has to decide about discovery or exclusion on the basis of counting the number of events. It is worthwhile to mention that, as we have only the leading order (LO) cross section for the background, there is quite a strong dependence of the latter upon the choice of the scale of α_s and also of the factorization scale. However, should the actual background normalization be calculated directly from the LHC data and, without going into further detail, one can legitimately assume a 5% uncertainty in our estimate of the background, by adding this error in quadrature to the estimated fluctuation of the latter, the requirement of 40 signal events for a 5σ discovery would go up to only 42 events, which hardly implies any modification to the mass reach and the event contours outlined above.

Before we conclude, let us compare our results with those

in Ref. [6]. The authors in [6] calculated the DY slepton pair production and decay to have a dilepton+missing energy signal in the final state. As already emphasized, the slepton production cross section via the DY channel is more than an order of magnitude higher than that via VBF for low slepton masses. However, the signal strength in the DY channel falls rapidly as the slepton mass increases, and ultimately the number of events becomes smaller than in the VBF channel. This is clearly evident from the slepton mass reach at the LHC ($\simeq$250 GeV) obtained in [6], whereas we have shown that the VBF channel can easily probe slepton masses well up to 500 GeV with more than 5σ significance over the leading backgrounds.

V. CONCLUSION

To summarize, we have investigated slepton pair production via VBF at the LHC. The cross section for slepton pair production along with two forward and backward jets has been estimated at the parton level. For low mass sleptons, the cross section in the VBF channel is much smaller than the one from DY production of sleptons. However, for higher slepton masses, the latter falls off quickly (below 1 fb) and the former becomes dominant while remaining sizable. The pair-production cross sections for both left and right sleptons have then been estimated, the former being marginally greater than the latter over the whole slepton mass range we have considered. We have then concentrated on slepton decays to the lightest neutralino, leading to two unlike-sign dileptons (of same flavor)+missing transverse momentum along with two forward and backward jets in the final state. Finally, we have devised simple kinematic cuts minimizing the leading SM backgrounds and found a rather large discovery potential up to slepton masses on the order of 500 GeV. Although our analysis was primarily based on the general MSSM, one can easily relate our results to the parameters of the MSUGRA scenario, as we have done ourselves in one instance. The overall conclusion is that our proposed signal should help in increasing the slepton mass reach at the LHC in a significant manner, in comparison to the scope of the previously considered DY channel.

ACKNOWLEDGMENTS

We thank the participants and organizers of the 7th Workshop on High Energy Physics Phenomenology (WHEPP-7) held at Allahabad, India, where this project was initiated. D.C. thanks the Dept. of Science & Technology, India for financial assistance under the Swarnajayanti Fellowship grant. A.D. and K.H. thank the Academy of Finland (project number 48787) for financial support. The work of B.M. is partially supported by the Board of Research in Nuclear Sciences, Government of India.

[1] J.D. Bjorken, Phys. Rev. D **47**, 101 (1993).
[2] R.N. Cahn and S. Dawson, Phys. Lett. **136B**, 196 (1984).
[3] A. Abbasabadi *et al.*, Phys. Rev. D **38**, 2770 (1998); Phys. Lett. B **213**, 386 (1988).
[4] R. Godbole and S. Rindani, Z. Phys. C **36**, 395 (1987); D. Rainwater and D. Zeppenfeld, J. High Energy Phys. **12**, 005 (1997); Phys. Rev. D **60**, 113004 (1999); D. Rainwater, D. Zeppenfeld, and K. Hagiwara, *ibid.* **59**, 014037 (1999); T. Plehn, D. Rainwater, and D. Zeppenfeld, *ibid.* **61**, 093005 (2000).
[5] A. Datta, P. Konar, and B. Mukhopadhyaya, Phys. Rev. D **65**, 055008 (2002); Phys. Rev. Lett. **88**, 181802 (2002).
[6] H. Baer *et al.*, Phys. Rev. D **49**, 3283 (1994); D. Denegri, L. Rurua, and N. Stepanov, CMS TN-1996/059; CMS Collaboration, CMS-TN-1998/006; S. Abdullin *et al.*, J. Phys. G **28**, 469 (2002); ATLAS Collaboration, ATL-PHYS-97-111, 1997.
[7] H. Baer, B.W. Harris, and M.H. Reno, Phys. Rev. D **57**, 5871 (1998); W. Beenakker *et al.*, Phys. Rev. Lett. **83**, 3780 (1999).
[8] S. Ambrosanio *et al.*, J. High Energy Phys. **01**, 014 (2001).
[9] J.F. Gunion, M. Herrero, and A. Mendez, Phys. Rev. D **37**, 2533 (1988).
[10] A. Datta and K. Huitu, Phys. Rev. D **67**, 115006 (2003).
[11] K. Hagiwara, H. Murayama, and I. Watanabe, KEK Report 91-11, 1991.
[12] H. Lai *et al.*, Phys. Rev. D **55**, 1280 (1997).
[13] See, for example, O. Eboli and D. Zeppenfeld, Phys. Lett. B **495**, 147 (2000).
[14] D. Rainwater, Ph.D. thesis, Wisconsin University, hep-ph/9908378.
[15] V. Khoze *et al.*, Eur. Phys. J. C **26**, 429 (2003).
[16] S. Moretti, J. Phys. G **28**, 2567 (2002).
[17] F. Maltoni and T. Stelzer, J. High Energy Phys. **02**, 027 (2003).
[18] See, for example, S.P. Martin, hep-ph/9709356.